

1 Remotely-sensed wind speed predicts soaring behaviour in a wide-  
2 ranging pelagic seabird

3

4 Rory Gibb<sup>1,2\*</sup>, Akiko Shoji<sup>3</sup>, Annette L. Fayet<sup>3</sup>, Chris M. Perrins<sup>4</sup>, Tim Guilford<sup>3</sup> and  
5 Robin Freeman<sup>1\*</sup>

6

7 <sup>1</sup>*Institute of Zoology, Zoological Society of London, Regent's Park, London NW1 4RY*

8 <sup>2</sup>*Centre for Biodiversity and Environment Research, Department of Genetics, Evolution and  
9 Environment, University College London, Gower Street, London, WC1E 6BT*

10 <sup>3</sup>*Oxford Navigation Group, Department of Zoology, University of Oxford, South Parks Road,  
11 Oxford, OX1 3PS, UK*

12 <sup>4</sup>*Edward Grey Institute, Department of Zoology, University of Oxford, South Parks  
13 Road, Oxford OX1 3PS, UK*

14

15 \* Corresponding authors: [rory.gibb.14@ucl.ac.uk](mailto:rory.gibb.14@ucl.ac.uk) and [robin.freeman@ioz.ac.uk](mailto:robin.freeman@ioz.ac.uk)

16

17 *This is a pre-copyedited, author-produced PDF of an article accepted for publication in the*  
18 *journal Journal of the Royal Society Interface following peer review. The version of record is*  
19 *not yet available but will be found on the journal's website from around September 2017.*

20

21 **Abstract**

22  
23 Global wind patterns affect flight strategies in many birds, including pelagic seabirds, many of  
24 which use wind-powered soaring to reduce energy costs during at-sea foraging trips and  
25 migration. Such long-distance movement patterns are underpinned by local interactions between  
26 wind conditions and flight behaviour, but these fine-scale relationships are far less well-  
27 understood. Here [we](#) show that remotely-sensed ocean wind speed and direction are highly  
28 significant predictors of soaring behaviour in a migratory pelagic seabird, the Manx shearwater  
29 (*Puffinus puffinus*). We used [high-frequency GPS tracking data \(10Hz\)](#) and statistical behaviour  
30 state classification to identify two energetic modes in at-sea flight, corresponding to flap-like and  
31 soar-like flight. We show that soaring is significantly more likely to occur in tailwinds and  
32 crosswinds above a wind speed threshold of around  $8\text{ms}^{-1}$ , suggesting that these conditions  
33 enable birds to reduce metabolic costs by preferentially soaring over flapping. Our results  
34 suggest a behavioural mechanism by which wind conditions may shape foraging and migration  
35 ecology in pelagic seabirds, and thus indicate that ~~climate change driven shifts in~~ wind patterns  
36 ~~shifts driven by climate change~~ could impact this and other species. They also emphasise the  
37 emerging potential of high-frequency GPS bi loggers to provide detailed quantitative insights  
38 into fine-scale flight behaviour in free-living animals.

39

40 **Keywords:** movement ecology, seabirds, tracking, remote sensing, wind, soaring

41

42

43

44

45

## 46 1. Introduction

47  
48 The effects of global-scale environmental variables (e.g. temperature, precipitation) on animal  
49 ecology are well-known, but similar relationships with wind have been much less extensively  
50 studied. Wind conditions affect phenology, migration routes, ecological interactions and foraging  
51 success in many volant animals including birds, bats and insects (e.g. [1–4]). Recent GPS  
52 tracking studies have shown that global winds affect long-distance patterns of foraging and  
53 migration behaviour in various wide-ranging bird species [5–8], however much less is known  
54 about the effect of more localised wind conditions. Understanding such fine-scale interactions  
55 between flight behaviour and the environment is key to understanding how individual  
56 behavioural responses to wind scale up to shape movement patterns at large spatial scales and  
57 over evolutionary time, such as the evolution of stable migration routes [8,9]. In a conservation  
58 context, such knowledge is also important to predict how shifts in atmospheric conditions under  
59 climate change [10–12] may impact many migratory birds.

60  
61 Pelagic seabirds are top marine predators that regularly travel hundreds ~~or thousands~~ of  
62 kilometres during foraging and migration [13], making them particularly reliant on ocean wind  
63 patterns [14–17]. During these journeys many albatrosses and shearwaters (Procellariiformes)  
64 engage in specialised modes of wind-powered soaring behaviour, thought to be metabolically  
65 less ~~metabolically~~ costly than flapping flight [18–20]. Data from GPS and accelerometer tags are  
66 now providing insights into soaring in free-living albatrosses and other birds [21–23], however  
67 much remains unknown about the fine-scale relationship between local winds and soaring  
68 behaviour. In this study we use very high-frequency GPS tracking (10Hz) to show that wind  
69 speed and direction, measured via satellite remote sensing, are highly significant predictors of  
70 soaring behaviour in a migratory pelagic seabird, the Manx shearwater (*Puffinus puffinus*). **Manx**

71 shearwaters are small (~400g), burrow nesting, pelagic seabirds. They are Amber listed in the  
72 UK [24] where most (~80%) of the global Manx shearwater population nests. They forage from  
73 breeding colonies around the UK coastline each summer before migrating to overwinter off  
74 southern Argentina, making an annual round trip of over 20,000km [9, 25–27].

75  
76 We tracked breeding adults during at-sea foraging trips using custom GPS loggers that record  
77 bursts of 3D location fixes at 10Hz, and distinguished flight behaviour from each burst's  
78 mechanical energy characteristics. A bird's total mechanical energy at any time consists of the  
79 two components *kinetic* (related to speed) and *gravitational potential* energy (related to altitude).  
80 During flight, total energy can increase either through flapping, when stored chemical energy is  
81 converted to power in the wing muscles, or through input from an external energy source, e.g.  
82 wind [28]. Relative changes to the kinetic and potential energy components are determined both  
83 by the magnitude of energy input and the bird's current mode of movement. Different flight  
84 behaviours therefore show markedly different patterns of mechanical energy change over time,  
85 which can be calculated from high-frequency 3D GPS positional data (e.g. [22]). During soaring,  
86 tracked albatrosses show large cyclical variations in both potential (derived from altitude) and  
87 kinetic energy (derived from ground speed) as they ascend and descend through the shear wind  
88 gradient above the sea surface [22]. Although Manx shearwaters are 'flap-glidors', mixing  
89 intermittent wingbeat pulses with gliding and soaring [13], we hypothesised that wind-powered  
90 soaring in this species would show similar variations in energy and ground speed.

91  
92 We therefore aimed to assess the prevalence of wind-powered soaring in Manx shearwaters and  
93 how this may vary under different environmental conditions. If, as might be expected, wind  
94 conditions play a role in how frequently soaring can occur, and soaring represents an  
95 energetically favourable mode of flight, then this has implications for the cost of movement

96 during travel and foraging. This can have knock-on effects upon how much effort is expended  
97 during reproduction, which has been demonstrated to impact breeding success in subsequent  
98 years [29]. Furthermore, quantifying the impacts of environmental conditions on the energetics  
99 of movement has potential implications for understanding the timing and success of migration  
100 and stopover [9]. This study also represents a proof of concept, demonstrating the potential of  
101 high-frequency GPS to analyse predictive relationships between movement and environmental  
102 conditions, with implications for understanding distribution, space-use and conservation of  
103 seabird species.

104

## 105 **2. Methods**

106

### 107 *2.1. GPS tracking procedure*

108

109 We tracked breeding adult birds during the chick-rearing season, between 12th and 25th August  
110 2012 at the study colony on Lundy Island, Devon, UK (51.1781° N, 4.6673° W). We deployed  
111 our own custom GPS loggers ([mataki.org](http://mataki.org) [30]) on 8 birds. Devices were positioned on the back  
112 above the bird's centre of gravity and attached to feathers with marine tape, ensuring that if  
113 loggers could not be retrieved they would loosen and fall off within 2-3 weeks (see details in  
114 [25,31]). Study individuals weighed between 415 and 470g, and complete mass of devices  
115 including tape was less than 17g, under 3.6% of body mass. To maximise the proportion of  
116 foraging trips recorded, devices were programmed to record 10Hz bursts of GPS fixes for ~~up to~~  
117 60 seconds, at 30 minute intervals. Each fix recorded latitude, longitude and altitude, so each  
118 discrete sequence of 10Hz fixes (hereafter '*burst*') forms a detailed track of the bird's movement  
119 through its environment. All loggers were retrieved from recaptured birds and data were  
120 downloaded for analysis. One bird remained in its burrow for the study duration, so at-sea GPS

121 tracks were obtained from 7 birds (Table 1). ~~These birds recorded 7~~Seven complete foraging  
 122 trips ~~were recorded from these birds~~, with durations of 17.1 to 53.5hrs (mean  $44.9 \pm 23.8$ hrs),  
 123 and 4 incomplete foraging trips during which the device battery expired before the bird returned  
 124 to the colony.  
 125

| ID | Number of bursts | Body mass before tracking (g) | Tracking time (hr) | Total distance (km) | Flap-like % | Soar-like % | Sitting % | Colony % | Wind speed (mean $\pm$ sd) ( $\text{ms}^{-1}$ ) |
|----|------------------|-------------------------------|--------------------|---------------------|-------------|-------------|-----------|----------|---|
| 1  | 114              | 445                           | 79                 | 625.1               | 21.9        | 26.3        | 35.1      | 16.7     | $11.05 \pm 1.6$                                 |
| 2  | 115              | 430                           | 85.8               | 483.7               | 11.3        | 9.6         | 72.2      | 6.9      | $6.54 \pm 3.59$                                 |
| 3  | 56               | 440                           | 46.8               | 282.6               | 17.8        | 25.0        | 51.8      | 5.3      | $10.97 \pm 2.52$                                |
| 4  | 33               | 470                           | 25.9               | 200.8               | 21.2        | 9.1         | 48.5      | 21.2     | $1.9 \pm 0.25$                                  |
| 5  | 44               | 465                           | 28.5               | 123.1               | 22.7        | 4.5         | 43.2      | 29.5     | $7.09 \pm 0.15$                                 |
| 6  | 101              | 450                           | 94.9               | 700.8               | 26.7        | 2.9         | 58.4      | 11.9     | $4.82 \pm 3.0$                                  |
| 7  | 96               | 440                           | 76.9               | 462.8               | 8.3         | 31.3        | 37.5      | 22.9     | $10.58 \pm 1.76$                                |

126  
 127 **Table 1:** Summary tracking statistics for all 7 birds, including proportion of recorded bursts  
 128 classified as soar-like, flap-like, sitting and colony-associated, and average wind speed (mean  $\pm$   
 129 sd) encountered during the tracking period.  
 130

131

## 132 2.2. Track processing and movement analysis

133

134 All analyses were carried out in R v. 3.1.2 [32]. Complete GPS tracks were filtered to exclude  
 135 fixes with erroneous timestamps and those derived using fewer than four satellites, the minimum  
 136 required for a precise three-dimensional location and time fix [25]. Each bird's track was split  
 137 into its constituent bursts and ~~each burst's the~~ median latitude and longitude ~~of each burst~~ were  
 138 assigned as its location. Since this study concerns at-sea activity, colony-associated bursts  
 139 (within 1500m radius around Lundy, n=84) were excluded, as were information-poor bursts of  
 140 fewer than 20 points (n=35), leaving a total of n=475 at-sea bursts. Within each burst we  
 141 calculated distance and ground speed (velocity with respect to Earth's surface) between

142 successive fixes. Fixes with speeds exceeding  $40 \text{ ms}^{-1}$  were excluded as likely GPS errors [25].

143 To reduce the effect of any small GPS positional errors or missed fixes, we smoothed ground

144 speed and altitude along each burst by applying a 15-point (1.5sec) rolling mean.

145

146 Following [23], from each fix's ground speed and altitude we calculated mechanical energy

147 components kinetic ( $E_K$ ), gravitational potential ( $E_P$ ) and total energy ( $E_T = E_K + E_P$ ), and also

148 mechanical power ( $P$ ), which measures the rate of  $E_T$  change across each between-fix time

149 interval. These describe a bird's in-flight mechanical energy relative to the earth's surface (as

150 inertial frame of reference), and their relative changes across a 60-second tracked burst describe

151 flight dynamics in detail [22]. Although not directly related to metabolic energy expenditure,

152 power values in excess of 0 indicate a net increase in mechanical energy over time, which could

153 either be due to metabolic energy input (from wing muscles) or from the wind [28]. There is an

154 upper limit to the power a bird can generate by flapping, therefore high power values and very

155 large variation in  $E_K$  and power are strongly suggestive of wind energy input [22]. Further detail

156 on track processing is provided in supplementary material (S1).

157

158 Tracking data are inherently statistically non-independent, with an animal's movement at any

159 time [being](#) influenced by its recent activities, internal state and environment [33,34]. However,

160 between-burst time intervals were sufficiently large (minimum 31.08min) to allow each to be

161 treated as functionally independent. We therefore compared bursts by calculating the following

162 summary parameters for each burst: (i) beeline distance (straight-line distance between burst start

163 and end points); (ii) mean ground speed (*'mean speed'*); (iii) standard deviation of kinetic energy

164 (*' $E_K$  variance'*); (iv) standard deviation of power (*'power variance'*); and (v) straightness index

165 (beeline distance divided by total path length), a measure of path tortuosity ranging from

166 completely straight (SI=1) to randomly oriented (SI=0) [35].

167  
 168 Clusters in the distribution of summary parameters corresponding to putative flight modes were  
 169 identified by fitting multivariate Gaussian mixture models (GMMs) by expectation-maximisation  
 170 (EM), using mclust v.4.4 [36,37]. GMMs estimate the probability of each observation belonging  
 171 to each cluster, and as such are a useful framework for identifying energetic modes from 60-  
 172 second bursts of tracked flight, which often contain mixtures of flap-powered and wind-powered  
 173 flight rather than single discrete behaviours. All variables were transformed to have mean 0 and  
 174 standard deviation 1 before model fitting.

175

### 176 *2.3. Modelling behavioural responses to environment*

177

178 Metop/ASCAT remotely-sensed wind data (24-hour averaged at 0.25° resolution) were obtained  
 179 from CERSAT (<http://www.ifremer.fr/cersat>). For each burst location this provided both total  
 180 wind speed and separate zonal and meridional components, from which we calculated wind  
 181 direction. Each burst's flight direction relative to wind (*'flight direction'*) was calculated as the  
 182 difference between burst beeline bearing and wind direction, and categorised as 'tailwind' (a  
 183 difference of 0° to 50°), 'crosswind' (50° to 130°) or 'headwind' (130° to 180°), following [13].

184 We also obtained remotely-sensed data for [sea surface chlorophyll \*a\* concentration \(CHL\)](#), [net](#)  
 185 [primary productivity \(NPP\)](#) and [sea surface temperature \(SST\)](#), to test possible relationships  
 186 between flight mode and ocean productivity as proxy for prey abundance (see supplementary  
 187 material S2). **CHL and SST from Aqua and Terra MODIS were obtained from NASA**  
 188 **OceanColor (4km, 8640 x 4320, 8-day composite, <http://oceancolor.gsfc.nasa.gov/cms/>). Aqua**  
 189 **and Terra values were averaged where both were available, and missing data values were**  
 190 **removed. Modelled NPP was obtained from Oregon State University Ocean Productivity (2160 x**  
 191 **4320, 8-day composite, <http://www.science.oregonstate.edu/ocean.productivity/>). We modelled**

192 relationships between flight mode, wind and ocean productivity using logistic mixed-effects  
 193 regression (lme4 v.1.1-7 [38]).

194

195

196

197

198

199

200

201

202

203

204

205

206

207

208

209

210

211

212

213

214

215

216

217

218

219

220

221

222

223

224

225

226

227

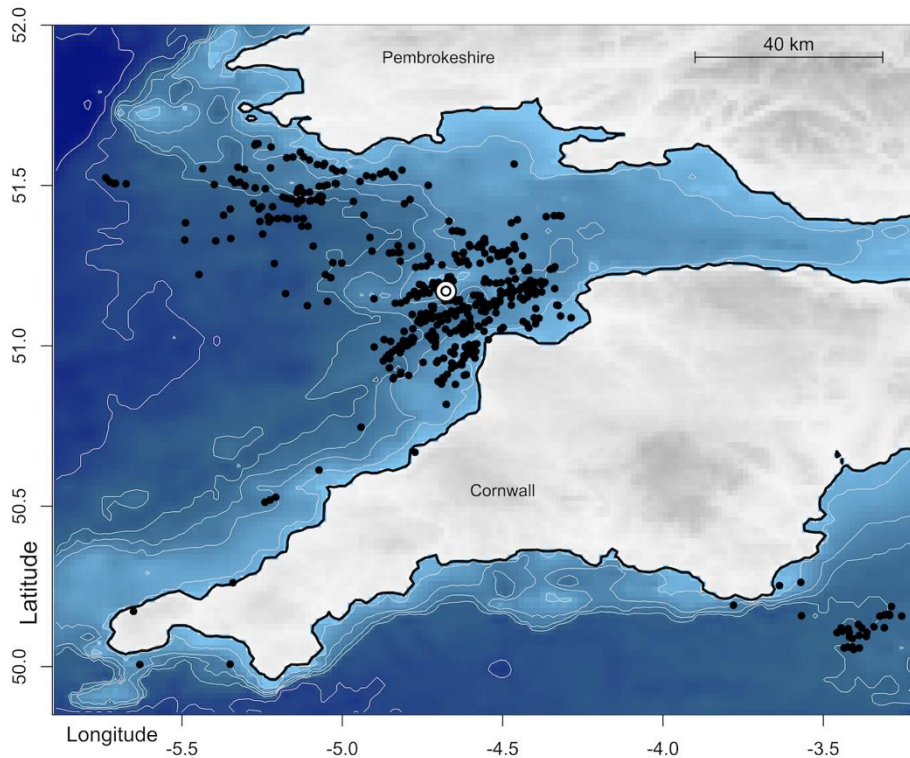


**Figure 1:** Distribution of Manx shearwaters foraging around Lundy Island (white circle), tracked between 12th and 25th August 2012 (n=7). Black points denote 60-second bursts of tracked movement (n=475) and are shown relative to the underlying bathymetry, accessed from National Oceanic and Atmospheric Administration (NOAA) via marmap [39].

### 3. Results

#### 3.1. Flight mode classification

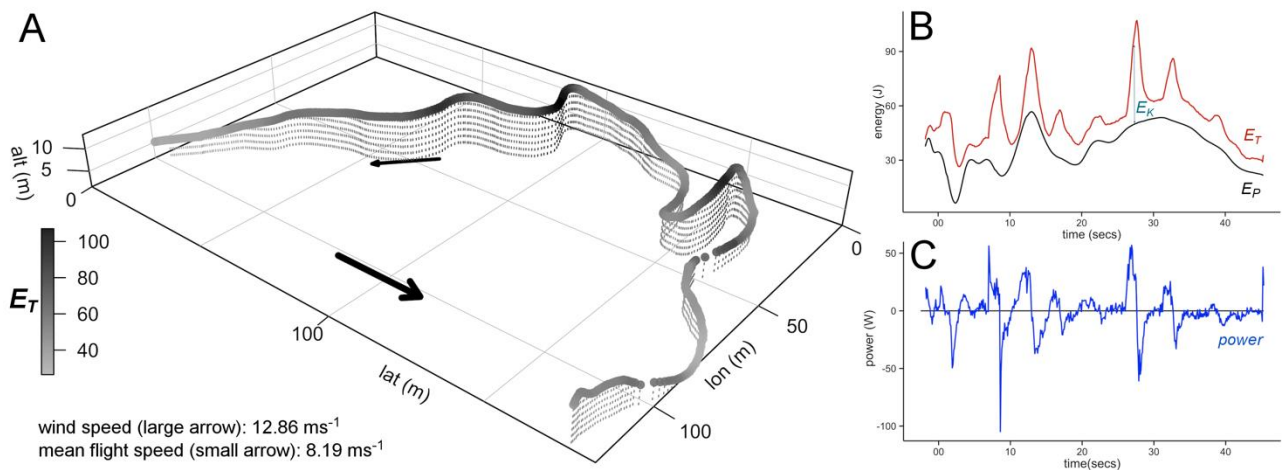
Foraging was mostly concentrated locally around Lundy and northwest towards Wales (Figure 1; mean distance from colony  $33.0 \pm 35.4$ km). Track processing yielded a final dataset of at-sea 10Hz bursts (n=475) (Figure 2; for more examples see supplementary material S4). Although most recorded for a full 60 seconds, some bursts were shorter due to device error (burst length

228 **mean 43.9sec, median 59.9sec**. We were only interested in bursts recorded during flight, so  
229 following [25], we first classified bursts as either in-flight (n=193) or sitting on sea surface  
230 (n=282) by fitting a two-component GMM to the bimodal distribution of mean speeds (BIC=-  
231 625.7, log-lik=-297.44; Figure S5). Flight bursts showed high mean speed ( $10.89 \pm 3.31 \text{ ms}^{-1}$ )  
232 while sitting bursts showed low mean speed and variance ( $1.33 \pm 0.61 \text{ ms}^{-1}$ ). Sitting bursts were  
233 excluded from subsequent analysis.

234  
235 For all flight bursts (n=193) we identified clusters in the distribution of mean speed, power  
236 variance and  $E_K$  variance by iteratively fitting trivariate GMMs with an increasing number of  
237 clusters. Although Bayesian Information Criterion (BIC) was maximised with a 3-component  
238 model, by far the greatest BIC increase was observed between 1 and 2 component models,  
239 identifying a clear knee-point [40]. We therefore selected a mixture of 2 ellipsoidal Gaussian  
240 components as most parsimonious (BIC=-1270.09, log-lik=-585.05, df=19). The first  
241 component's high speed and low energetic variance was consistent with powered flapping flight,  
242 while the second component showed high speed and high energetic variance, consistent with  
243 wind-powered soaring (Figure 3a). Each flight burst was classified to either flap-like (n=115) or  
244 soar-like (n=78) by maximum probability. Bursts classified with under 95% probability (*low-*  
245 *certainty bursts*, n=74) were of intermediate energetic variance and visual inspection suggested  
246 that most contained mixtures of flight modes, although the GMM classified the majority as flap-  
247 like (n=55). **However, the resolution of the available environmental covariates meant that it**  
248 **would not be possible to resolve finer-scale relationships between the environment and within-**  
249 **burst variations in flight mode. We therefore decided to classify bursts in their entirety to either**  
250 **flap-like or soar-like for subsequent analyses.**

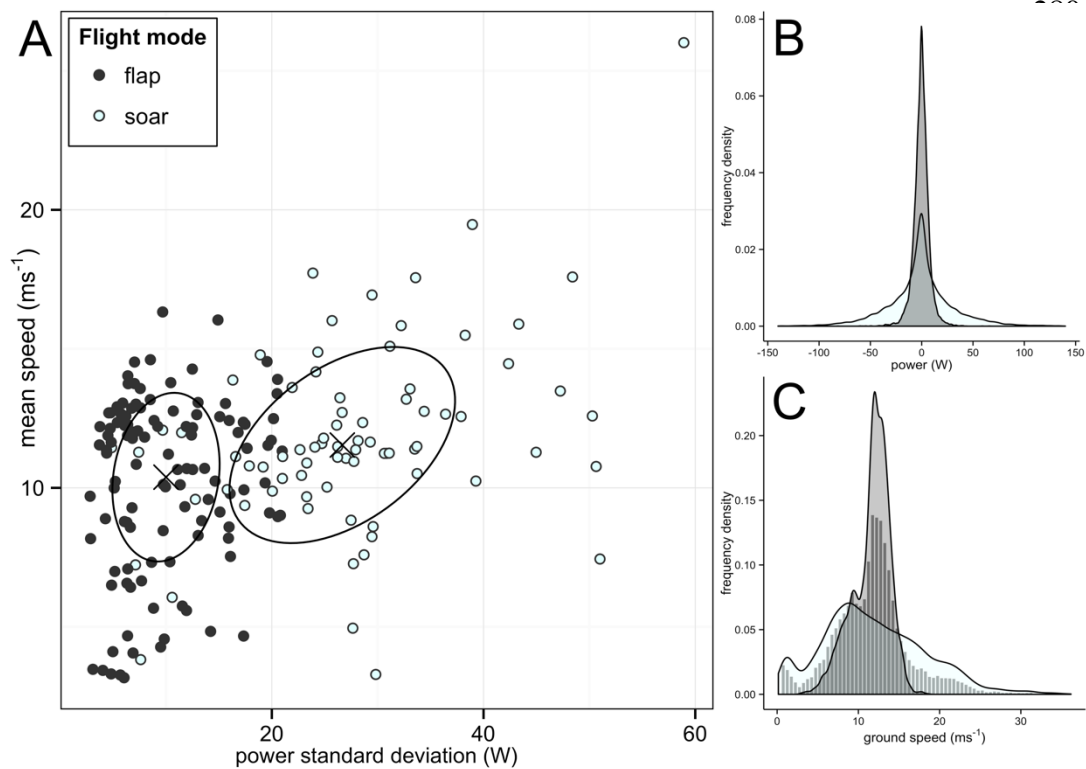
251

252 Summary energetic parameter values for flap-like and soar-like bursts classified with over 95%  
 253 probability (*high-certainty bursts*) are reported in Table 2. High-certainty flap-like and soar-like  
 254 bursts contained markedly different distributions of fine-scale in-flight power and ground speed  
 255 (Figure 3b-c). Energetic dynamics within soar-like bursts generally consisted of large oscillations  
 256 in power, often due to rapid  $E_K$  gains. There were large differences in the amount of time that  
 257 different individuals spent engaging in different behaviours (Table 1). There were overlaps in  
 258 foraging areas between birds, but no obvious visible spatial trends in the at-sea distribution of  
 259 flap-like and soar-like flight (Figure S3).  
 260



261  
 262 **Figure 2:** A high-frequency GPS flight burst. The bird's 3D path through space (A) is shown  
 263 with track shaded by total mechanical energy ( $E_T$ ), with arrows showing wind direction (large)  
 264 and flight direction (small). Separate graphs show mechanical energy components  $E_T$ ,  $E_P$  and  $E_K$   
 265 (B) and power (C) against time. This burst contains both low-power flapping and spikes in power  
 266 suggesting wind energy input.  
 267  
 268  
 269  
 270  
 271  
 272  
 273  
 274  
 275  
 276  
 277  
 278

279



290 **Figure 3:** Energetic characteristics of flap-like and soar-like flight. [The \(A\) relationship](#)  
 291 [Relationship](#) between burst summary parameters power variance and mean speed, [is shown in](#)  
 292 [\(A\)](#)-with ellipses showing modelled Gaussian components (mean+sd). [\(B\)](#) Density curves show  
 293 within-burst distributions of fine-scale power (B) and ground speed (C) for flap-like (grey) and  
 294 soar-like flight (white), produced by combining 10Hz points from all bursts classified to either  
 295 mode with over 95% probability. The distribution of ground speeds across all flight bursts (both  
 296 flap-like and soar-like) was trimodal (histogram in C).

297

298

299

300

| Flight mode | number of bursts | mean ground speed (ms <sup>-1</sup> ) | power variance (W) (*) | $E_K$ variance (J) (*) | beeline distance (m) | straightness index (**) |
|-------------|------------------|---------------------------------------|------------------------|------------------------|----------------------|-------------------------|
| Flap-like   | 60               | 11.46 ± 2.23                          | 7.22 ± 2.63            | 4.98 ± 2.74            | 422.3 ± 268.3        | 0.88 ± 0.12             |
| Soar-like   | 59               | 11.97 ± 3.84                          | 30.62 ± 10.5           | 27.29 ± 10.68          | 418.0 ± 299.5        | 0.72 ± 0.25             |

301

302 **Table 2:** Summary [mechanical energy movement and energetic](#) characteristics of bursts classified  
 303 to flap-like and soar-like with over 95% probability (n=119). Values reported are mean ± sd.  
 304 Asterisks denote a significant difference between flap-like and soar-like bursts ( $p < 0.0001$ ),  
 305 tested using either two-sided t-test (\*) or Wilcoxon sum-ranks (\*\*).

306

307

308

309 *3.2. Environmental predictors of soaring*

310

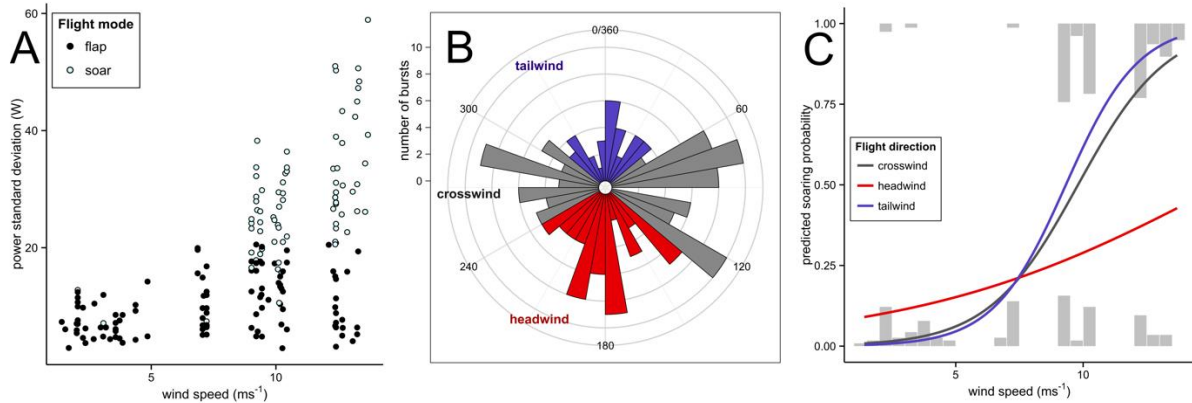
311 Wind speed data were accessed for 189 bursts (data for 4 bursts were missing from the  
 312 METOP/ASCAT dataset, possibly because of cloud cover). Tracked birds encountered wind  
 313 speeds between 1.41 and 13.69 ms<sup>-1</sup>, with each bird experiencing a range of wind speeds during  
 314 tracking (Table 1; Figure S10). Wind speed had a clear strong effect on power variance, with  
 315 soar-like bursts with high power variance almost exclusively observed in winds above 8 ms<sup>-1</sup>  
 316 (Figure 4a). Mean ground speeds were mostly concentrated between 11 and 15 ms<sup>-1</sup> in low  
 317 winds, becoming more variable at higher wind speeds (Figure S9). Birds were more often  
 318 recorded flying in crosswind (n=99) than headwind (n=57) or tailwind (n=33) (Figure 4b).

319

320 We modelled the relationship between wind speed, flight direction and flight mode using logistic  
 321 mixed-effects regression, including an interaction between wind speed and flight direction and  
 322 including individual and day as random effects (n=189, AIC=204.1, model outputs are reported  
 323 in supplementary materials). Model deviance was significantly reduced with wind speed and  
 324 flight direction included as predictors, compared to an intercept-only null model ( $\Delta$ AIC=19.5;  
 325  $\chi^2=29.5$ , null-residual deviance 217.57–188.11, df=5, p<0.0001). The model showed a highly  
 326 significant effect of wind speed on flight mode, with likelihood of soaring increasing at higher  
 327 wind speeds (Figure 4bFigure 4c). There was also a significant interaction between wind speed  
 328 and flight direction, with soaring occurring less frequently in strong headwinds than in tailwinds  
 329 or crosswinds (for separate plots for each flight direction, see supplementary material). The  
 330 strength and significance of both these relationships increased and model fit improved when low-  
 331 certainty bursts were excluded (n=119, AIC=93.9, residual deviance=77.9). The second model  
 332 additionally showed a significant effect of flight direction on flight mode, with reduced soaring

333 in headwind compared to crosswind and tailwind. We found no significant relationships between  
 334 flight mode and oceanic productivity (supplementary material S2).

335



336

337

338 **Figure 4:** The relationship between flight and wind conditions, for all flight bursts for which  
 339 wind data were available ( $n=189$ ). (A) Relationship between wind speed and burst power  
 340 variance, with flap-like bursts shown in black and soar-like bursts in white. (B) Histogram of the  
 341 per-burst difference in degrees between the bird's flight direction (beeline bearing) and wind  
 342 direction, where a value of  $0^\circ$  denotes no difference (i.e. flight direction is the same as wind  
 343 direction). For modelling, flight direction was categorised as headwind (shown in red),  
 344 crosswind (grey) or tailwind (blue). (C) Wind speed is a highly significant predictor of soar-like  
 345 flight (logistic mixed-effects regression controlling for individual and day), with soaring less  
 346 likely to occur in strong headwind than tailwind or crosswind. Grey histograms show density of  
 347 wind speeds for all bursts classified as either flap-like (bottom) or soar-like (top).

348

349

350

#### 351 4. Discussion

352

353 Ocean wind patterns are important drivers of seabird ecology and evolution [13,41], and recent  
 354 research integrating information from multiple bilogger types has revealed that winds are exert  
 355 a key-major influence on timing and distribution of foraging and migration in many species  
 356 [1,8,14,15]. The relationship we demonstrate between flight behaviour and local wind conditions  
 357 illuminates some of the behavioural mechanisms that underpin these large-scale patterns~~Our~~  
 358 ~~results show a relationship between flight behaviour and local wind conditions that sheds light on~~  
 359 ~~the behavioural mechanisms underpinning these larger-scale ecological trends.~~ Crosswinds and

360 tailwinds above a wind speed threshold of around  $8\text{ms}^{-1}$  are highly significant predictors of soar-  
361 like behaviour in foraging Manx shearwaters. While we emphasise that these results come from a  
362 population sample of 7 individuals, they support the inference that suitable wind conditions  
363 enable birds to engage in soar-like flight, which is likely to reduce overall energy costs during  
364 | journeys. ~~While s~~Statistical behaviour state classification is increasingly used to analyse animal  
365 | tracking data [26,33,42]. ~~However,~~ to our knowledge this is the first time such an approach has  
366 | been used to both identify distinct modes of flight behaviour and demonstrate their predictive  
367 | relationship to environmental conditions.

368

#### 369 *4.1. Tracking and modelling of flight behaviour*

370

371 The effect of tags on study animals is a key consideration in tracking research. Previous tests  
372 with devices of equal weight reported minimal impacts on movement and reproductive success  
373 in Manx shearwaters [42], however we tracked movement at much finer temporal resolution than  
374 any previous study, and it is impossible to rule out the effects that a device weighing up to 4% of  
375 body mass could have on behaviour (e.g. [43]). Nonetheless, we observed the same responses to  
376 wind speed across several individuals that encountered both low and high winds during tracking.  
377 We suggest that although tag weight may impact flight to some degree, this is unlikely to  
378 significantly alter overall behavioural trends.

379

380 Using mean ground speed, kinetic energy ( $E_K$ ) and power as variables in the GMM offered  
381 several advantages for distinguishing wind-powered from flap-powered flight behaviour.  
382 Although the relative 3D positional accuracy of successive GPS fixes is very high, absolute GPS  
383 accuracy is more reliable horizontally (used to calculate ground speed and  $E_K$ ; absolute error of  $\pm$   
384 2.5m) than vertically (used to calculate potential energy  $E_P$ ). Visually inspecting all flight bursts

385 showed no abrupt changes in altitude that were obviously artefacts, however we opted to exclude  
 386 absolute  $E_P$  values (which are derived from absolute altitude) from the GMM in order to  
 387 minimise any potential effects of GPS error. Mechanical power measures the rate of energy  
 388 change across each between-fix time interval  $t$  ( $P = (\Delta E_K + \Delta E_P) / t$ ), so by including power  
 389 (derived from change in altitude) as an input variable we ensured that the GMM still  
 390 incorporated relative changes in  $E_P$ , an important aspect of soaring flight. For additional model  
 391 validation we also independently hand-classified bursts as soar-like or flap-like based on visual  
 392 inspection of their shape, and the results closely resembled model outputs (Figure S7), improving  
 393 our confidence that the clusters identified by the GMM correspond to these behaviours.

394  
 395 The GMM clearly distinguished ~~majority bursts that contained mostly~~ flap-like ~~and or~~ soar-like  
 396 ~~bursts~~ movement, due to their markedly different mechanical characteristics. However, it  
 397 appeared slightly biased towards classifying low-certainty bursts (those classified with under  
 398 95% probability) as flap-like (n=55) rather than soar-like (n=17), despite visual inspection  
 399 suggesting that most were mixed-mode. These intermediate energy bursts mostly occurred in  
 400 wind speeds above the soaring threshold (Figure S8) suggesting that our models may slightly  
 401 underestimate use of soaring in wind speeds above  $8 \text{ ms}^{-1}$ . This emphasises that although a  
 402 behavioural state framework is a useful abstraction for modelling relationships between flight  
 403 mode and environment, Manx shearwater flight is complex and responsive to local heterogeneity  
 404 in wind and wave conditions. 60-second tracked flight bursts exist on a continuum of mixed  
 405 behaviours, ranging from mostly flap-like to mostly soar-like (e.g. Figure 2). This variability  
 406 reflects the smaller wingspan and flap-gliding flight of this species compared to that of large  
 407 soaring specialists such as albatrosses, which travel long distances without flapping their wings.  
 408 Soar-like bursts occasionally showed regular  $E_P$  and  $E_K$  oscillations resembling those observed in  
 409 albatrosses, albeit with shorter soar cycle lengths (5sec compared to 15sec) [22], however such

410 stereotyped movement was relatively uncommon (see supplementary material S4). **The**  
 411 **resolution of the available environmental covariates meant that it was not feasible to model the**  
 412 **effect of environment on within-burst variability in flight behaviour. However, in future, either**  
 413 **accessing wind data at a higher spatiotemporal resolution (e.g. collected using on-animal tags) or**  
 414 **recording much longer high-frequency GPS bursts (e.g. 5-10 minutes or above) could potentially**  
 415 **facilitate analysis of the effect of wind on flight behaviour at an even finer scale.**

416

#### 417 *4.2. Flap-like and soar-like flight characteristics*

418

419 Birds engaging in powered flapping flight are predicted to minimise net energy expenditure by  
 420 travelling close to maximum range velocity ( $V_{mr}$ ), the speed at which maximum distance is  
 421 covered per unit of fuel [28]. Previous studies tracked Manx shearwaters at mean ground speeds  
 422 of 10–11  $\text{ms}^{-1}$ , slower than their estimated  $V_{mr}$  of 14  $\text{ms}^{-1}$ , suggesting some use of wind while  
 423 travelling [25,27]. Our results confirm this, and show that soar-like flight enables shearwaters to  
 424 travel at equivalent mean ground speeds as flapping (Table 2). Within flap-like bursts the highest  
 425 density of ground speeds occurred between 12 and 14  $\text{ms}^{-1}$  ~~Within flap-like bursts we observed a~~  
 426 ~~clear ground speed peak between 12 and 14  $\text{ms}^{-1}$~~ -(Figure 3c), with birds apparently maximising  
 427 efficiency by travelling close to  $V_{mr}$ . The relationship between ground speed and airspeed varies  
 428 with flight direction relative to wind; we hypothesise that birds maintain airspeeds close to  $V_{mr}$   
 429 throughout flapping, and that much of the observed within-burst variability in ground speed is  
 430 due to birds flying with or against the wind, as indeed is the broader distribution of mean ground  
 431 speeds observed in high winds (Figure S9).

432

433 In contrast, during soar-like flight regular kinetic energy boosts from the wind generate power  
 434 levels far exceeding those available through flapping alone (Figure 3b), with maximum available

435 power appearing to increase as a function of wind speed (Figure 4a). Accelerating and slowing  
436 repeatedly as they change flight path and body orientation relative to wind, soaring birds cover a  
437 far broader range of ground speeds (Figure 3c) along significantly more tortuous flight paths  
438 (Table 2). Soar-like flight in Manx shearwaters involves more flapping activity than in  
439 albatrosses [13], whose metabolic costs while soaring are extremely low [18]. Nonetheless, we  
440 find that soaring shearwaters cover equivalent distances as in flap-like flight (Table 2) while  
441 spending much more time flying at closer to their estimated minimum power velocity ( $V_{mp}$ ) of  
442  $7.5 \text{ ms}^{-1}$  (Figure 3c), which strongly suggests that energy expenditure is lower during soar-like  
443 flight. The second smaller peak between 0 and  $2.5 \text{ ms}^{-1}$  emphasises the distinction between  
444 ground speed and airspeed; it corresponds to phases during soaring when birds ascend into  
445 oncoming wind, sharply decreasing in ground speed but simultaneously increasing in airspeed  
446 [22]. Birds were also more likely to soar in suitably strong tailwinds and crosswinds than  
447 headwinds, although the relative coarseness of our wind data (24-hour averaged vectors) means  
448 that these categorised directions may be inexact. This nonetheless makes intuitive sense, since  
449 soaring against strong headwind is both time-inefficient and metabolically costly [18,20].  
450  
451 More broadly, these insights emphasise the emerging potential of high-frequency GPS  
452 biologgers, either solo or paired with other sensor types [20,44], as tools for studying fine-scale  
453 movement behaviour in wild animals. Tri-axial accelerometers are typically used to quantify  
454 metabolic energy expenditure in tracked animals (e.g. [45,46]). However, since these measure  
455 body acceleration rather than an individual's position in space they can present challenges for  
456 studying soaring and gliding in birds, in which body posture often remains relatively fixed and  
457 much muscle work is isometric [44]. In future, combining high-resolution GPS with co-deployed  
458 accelerometer tags would enable more precise estimation of the relative metabolic costs of

459 different flight modes in this and other bird species, providing even more detailed insights into  
460 dynamic relationships between flight behaviour and the local environment.

461

#### 462 *4.3. Ecological relevance and future directions*

463

464 Global wind patterns affect migration strategies in many ~~migratory~~ birds [6,7,14] ~~and as well as~~  
465 ~~affecting the~~ foraging ecology ~~in of~~ pelagic seabirds [1,8]. Breeding and migration success may  
466 depend on minimising energy costs during these trips [1,28]. Our results support the inference  
467 that soaring in tailwinds and crosswinds above an  $8\text{ms}^{-1}$  threshold enables Manx shearwaters to  
468 reduce flight energy expenditure, and therefore suggest a local-scale behavioural mechanism by  
469 which the wind conditions experienced by birds during flight modulate the net cost of at-sea  
470 journeys. Wind conditions are therefore likely to affect route choice, for example sufficiently  
471 high speed crosswinds and tailwinds may provide low-cost soaring corridors to foraging areas.  
472 **This may contribute to the costs of foraging during reproduction, and may be an important factor**  
473 **to consider in future analysis of carry-over effects, e.g. [29]. Such a mechanism may also**  
474 underpin some of the considerable variety in foraging routes observed during several years'  
475 tracking of Manx shearwaters around the UK [27], as well as the flexible route choice strategies  
476 of other seabirds in response to wind [15,16]. Our data provide some support for this, in that the  
477 tracked birds travelling furthest northwest towards Wales were those that encountered the  
478 strongest winds and soared the most (Table 1).

479

480 Migratory birds are predicted to evolve migration strategies that minimise energetic costs [28].  
481 Following favourable conditions for soaring may be one behavioural mechanism by which long-  
482 term trends in oceanic wind patterns, including the persistence of stable atmospheric features,  
483 affect the evolution of migration routes and timing in the Manx shearwater and other seabirds

484 [8]. By identifying the wind conditions that favour soar-like flight, our results therefore present  
485 opportunities for a more predictive approach to understanding seabird life histories. We suggest  
486 that a future research direction, applying our model outputs, would be to combine global-scale  
487 wind data with the multiple years of geocator and GPS migration tracks now collected for this  
488 species [26,27], in order to further ~~understand~~ assess how local behavioural responses to wind  
489 influence its global spatial distribution and migratory routes. **Such an approach may also have  
490 conservation management implications for this and other seabirds. For example, although Manx  
491 shearwaters are generally considered low risk for collision with offshore wind turbines due to  
492 their relatively low-altitude flight [47], applying similar methods to assess the predictive  
493 relationship between wind conditions, flight behaviour and route choice in other, more  
494 vulnerable species may assist in predicting regions of present and future collision risk.**

495  
496 Our results also suggest that climate change-driven wind pattern shifts [10] have the potential to  
497 affect the costs of long-distance journeys in this species. Recent wind changes in the Southern  
498 Ocean have affected foraging routes and life history traits in wandering albatrosses [1],  
499 suggesting fitness impacts but also some behavioural plasticity in response to changing  
500 atmospheric conditions. However, as much smaller birds reliant on favourable winds for both  
501 foraging and migration [5], Manx shearwaters may be highly sensitive to such changes. If future  
502 global wind pattern shifts result in either increased energy expenditure during flight or extended  
503 travel times while at sea, this could have long-term population impacts on survival and  
504 reproductive success [8]. Similar impacts ~~could~~ may also be expected ~~for other~~ in other pelagic  
505 seabird species, whose populations are already in global decline due to human impacts on the  
506 marine environment [48].

507

508 **Conclusions**

509  
510 Data from on-board biologgers are fast improving our understanding of free-living animal  
511 movement. Using high-frequency GPS, here we have shown for the first time that wind speed,  
512 measured via satellite remote sensing, is an accurate predictor of soar-like flight in a wide-  
513 ranging pelagic seabird. Tailwinds and crosswinds above an  $8 \text{ ms}^{-1}$  wind speed threshold predict  
514 significantly increased likelihood of soaring flight. Both wind speed and direction are therefore  
515 likely to modulate flight costs during at-sea trips, suggesting a mechanism by which oceanic  
516 wind conditions could affect population-level foraging and migration strategies in this and other  
517 species. Our results highlight that high-frequency GPS should be considered within an emerging  
518 toolbox of tracking technologies that enable detailed quantitative study of the interactions  
519 between animal movement and the environment.

520

#### 521 **Ethics statement**

522

523 Research took place under review by the British Trust for Ornithology Unconventional Methods  
524 Panel (permit C/5311) and the University of Oxford's Local Ethical Review Process.

525

#### 526 **Data accessibility**

527

528 Data and code are archived on Figshare (<https://figshare.com/s/bd14e3a32e3ad340e323>). Link is  
529 private but will be made public on acceptance of manuscript.

530

#### 531 **Competing interests**

532

533 The authors have no competing interests.

534

535 **Authors' contributions**

536

537 R.G. and R.F. conceived the paper, R.F. and A.S. collected the data, and R.G. and R.F. analysed  
538 the data. All authors contributed to writing the manuscript.

539

540 **Acknowledgements**

541

542 Thanks to Igor Boczarow for assistance during data collection in the field, and to Chris Carbone  
543 and Rachel Lane. [We also thank our two reviewers for their helpful comments on the first](#)  
544 [version of this manuscript.](#)

545

546 **Funding**

547

548 This work was funded by the Lundy Field Society, Microsoft Research Cambridge, the  
549 Department of Zoology of Oxford University and the RSPB. A.L.F. was also funded by  
550 scholarships from the Biotechnology and Biological Sciences Research Council grant  
551 ATGAAB9, Microsoft Research Cambridge, the British Council Entente Cordiale Scheme, the  
552 Mary Griffiths Foundation, and an award from the British Federation for Women Graduates.

553

554 **Supplementary material**

555

556 Please see electronic supplementary materials PDF document.

557

558 **References**

559

560 1. Weimerskirch, H., Louzao, M., Grissac, S. de & Delord, K. 2012 Changes in wind pattern  
561 alter albatross distribution and life-history traits. *Science* **335**, 211–214.

562 (doi:10.1126/science.1210270)

563 2. Krauel, J. J., Westbrook, J. K. & McCracken, G. F. 2015 Weather-driven dynamics in a  
564 dual-migrant system: moths and bats. *J. Anim. Ecol.* **84**, 604–614. (doi:10.1111/1365-

565 2656.12327)

566 3. Chapman, J. W., Reynolds, D. R. & Wilson, K. 2015 Long-range seasonal migration in  
567 insects: mechanisms, evolutionary drivers and ecological consequences. *Ecol. Lett.* **18**,

568 287–302. (doi:10.1111/ele.12407)

569 4. Kranstauber, B., Weinzierl, R., Wikelski, M. & Safi, K. 2015 Global aerial flyways allow  
570 efficient travelling. *Ecol. Lett.* **18**, 1338–1345. (doi:10.1111/ele.12528)

571 5. González-Solís, J., Felicísimo, A., Fox, J. W., Afanasyev, V., Kolbeinsson, Y. & Muñoz,  
572 J. 2009 Influence of sea surface winds on shearwater migration detours. *Mar. Ecol. Prog.*

573 *Ser.* **391**, 221–230. (doi:10.3354/meps08128)

574 6. Klaassen, R. H. G., Hake, M., Strandberg, R. & Alerstam, T. 2011 Geographical and  
575 temporal flexibility in the response to crosswinds by migrating raptors. *Proc. R. Soc. B*

576 **278**, 1339–46. (doi:10.1098/rspb.2010.2106)

577 7. Vidal-Mateo, J., Mellone, U., Lopez-Lopez, P., La Puente, J. De, Garcia-Ripolles, C.,  
578 Bermejo, A. & Urios, V. 2016 Wind effects on the migration routes of trans-saharan

579 soaring raptors: geographical, seasonal, and interspecific variation. *Curr. Zool.* **62**, 89–97.

580 (doi:10.1093/cz/zow008)

581 8. Weimerskirch, H., Bishop, C., Jeanniard-du-Dot, T., Prudor, A. & Sachs, G. 2016 Frigate  
582 birds track atmospheric conditions over months-long transoceanic flights. *Science* **353**,

583 74–78. (doi:10.1126/science.aaf4374)

- 584 9. Guilford, T., Meade, J., Willis, J., Phillips, R. A., Boyle, D., Roberts, S., Collett, M.,  
585 Freeman, R. & Perrins, C. M. 2009 Migration and stopover in a small pelagic seabird, the  
586 Manx shearwater *Puffinus puffinus*: insights from machine learning. *Proc. R. Soc. B* **276**,  
587 1215–23. (doi:10.1098/rspb.2008.1577)
- 588 10. Young, I. R., Zeiger, S. & Babanin, A. V. 2011 Global trends in wind speed and wave  
589 height. *Science* **332**, 451–455.
- 590 11. McVicar, T. R. et al. 2012 Global review and synthesis of trends in observed terrestrial  
591 near-surface wind speeds: implications for evaporation. *J. Hydrol.* **416–417**, 182–205.  
592 (doi:10.1016/j.jhydrol.2011.10.024)
- 593 12. IPCC Core Writing Team, Pachauri, R. K. & Meyer, L. 2014 *Climate Change 2014:*  
594 *Synthesis Report. Contribution of Working Groups I, II and III to the Fifth Assessment*  
595 *Report of the Intergovernmental Panel on Climate Change. IPCC, Geneva, Switzerland.*
- 596 13. Spear, L. B. & Ainley, D. G. 1997 Flight behaviour of seabirds in relation to wind speed  
597 and direction. *Ibis (Lond. 1859)*. **139**, 234–251. (doi:10.1111/j.1474-  
598 919X.1997.tb04620.x)
- 599 14. Felicísimo, Á. M., Muñoz, J. & González-Solis, J. 2008 Ocean surface winds drive  
600 dynamics of transoceanic aerial movements. *PLoS One* **3**, e2928.  
601 (doi:10.1371/journal.pone.0002928)
- 602 15. Paiva, V. H., Guilford, T., Meade, J., Geraldes, P., Ramos, J. A. & Garthe, S. 2010 Flight  
603 dynamics of Cory's shearwater foraging in a coastal environment. *Zoology* **113**, 47–56.  
604 (doi:10.1016/j.zool.2009.05.003)
- 605 16. Tarroux, A. et al. 2016 Flexible flight response to challenging wind conditions in a  
606 commuting Antarctic seabird: do you catch the drift? *Anim. Behav.* **113**, 99–112.  
607 (doi:10.1016/j.anbehav.2015.12.021)
- 608 17. Kogure, Y., Sato, K., Watanuki, Y., Wanless, S. & Daunt, F. 2016 European shags

- 609 optimize their flight behavior according to wind conditions. *J. Exp. Biol.* **219**, 311–318.  
 610 (doi:10.1242/jeb.131441)
- 611 18. Weimerskirch, H., Guionnet, T., Martin, J., Shaffer, S. A. & Costa, D. P. 2000 Fast and  
 612 fuel efficient? Optimal use of wind by flying albatrosses. *Proc. R. Soc. B* **267**, 1869–74.  
 613 (doi:10.1098/rspb.2000.1223)
- 614 19. Pennycuik, C. J. 2002 Gust soaring as a basis for the flight of petrels and albatrosses  
 615 (Procellariiformes). *Avian Sci.* **2**, 1–12.
- 616 20. Spivey, R. J., Stansfield, S. & Bishop, C. M. 2014 Analysing the intermittent flapping  
 617 flight of a Manx Shearwater, *Puffinus puffinus*, and its sporadic use of a wave-meandering  
 618 wing-sailing flight strategy. *Prog. Oceanogr.* **125**, 62–73.  
 619 (doi:10.1016/j.pocean.2014.04.005)
- 620 21. Halsey, L. G., Portugal, S. J., Smith, J. A., Murn, C. P. & Wilson, R. P. 2009 Recording  
 621 raptor behavior on the wing via accelerometry. *J. F. Ornithol.* **80**, 171–177.  
 622 (doi:10.1111/j.1557-9263.2009.00219.x)
- 623 22. Sachs, G., Traugott, J., Nesterova, A. P. & Bonadonna, F. 2013 Experimental verification  
 624 of dynamic soaring in albatrosses. *J. Exp. Biol.* **216**, 4222–32. (doi:10.1242/jeb.085209)
- 625 23. Sachs, G., Traugott, J., Nesterova, A. P., Dell’Omo, G., Kümmeth, F., Heidrich, W.,  
 626 Vyssotski, A. L. & Bonadonna, F. 2012 Flying at no mechanical energy cost: disclosing  
 627 the secret of wandering albatrosses. *PLoS One* **7**, e41449.  
 628 (doi:10.1371/journal.pone.0041449)
- 629 24. Eaton, M. A., Brown, A. F., Hearn, R., Noble, D. G., Musgrove, A. J., Lock, L., Stroud,  
 630 D. & Gregory, R. D. 2015 Birds of conservation concern 4: the population status of birds  
 631 in the United Kingdom, Channel Islands and Isle of Man. *Br. Birds* **108**, 708–746.
- 632 25. Guilford, T. C., Meade, J., Freeman, R., Biro, D., Evans, T., Bonadonna, F., Boyle, D.,  
 633 Roberts, S. & Perrins, C. M. 2008 GPS tracking of the foraging movements of Manx

- 634 Shearwaters *Puffinus puffinus* breeding on Skomer Island, Wales. *Ibis (Lond. 1859)*. **150**,  
 635 462–473. (doi:10.1111/j.1474-919X.2008.00805.x)
- 636 26. Freeman, R., Dean, B., Kirk, H., Leonard, K., Phillips, R. A., Perrins, C. M. & Guilford,  
 637 T. 2013 Predictive ethoinformatics reveals the complex migratory behaviour of a pelagic  
 638 seabird, the Manx Shearwater. *J. R. Soc. Interface* **10**, 20130279.  
 639 (doi:10.1098/rsif.2013.0279)
- 640 27. Dean, B., Kirk, H., Fayet, A., Shoji, A., Freeman, R., Leonard, K., Perrins, C. M. &  
 641 Guilford, T. 2015 Simultaneous multi-colony tracking of a pelagic seabird reveals cross-  
 642 colony utilization of a shared foraging area. *Mar. Ecol. Prog. Ser.* **538**, 239–248.  
 643 (doi:10.3354/meps11443)
- 644 28. Pennycuik, C. J. 1969 The mechanics of bird migration. *Ibis (Lond. 1859)*. **111**, 525–556.  
 645 (doi:10.1111/j.1474-919X.1969.tb02566.x)
- 646 29. Fayet, A. L., Freeman, R., Shoji, A., Kirk, H. L., Padget, O., Perrins, C. M., Guilford, T.  
 647 & Verhulst, S. 2016 Carry-over effects on the annual cycle of a migratory seabird: an  
 648 experimental study. *J. Anim. Ecol.* **85**, 1516–1527. (doi:10.1111/1365-2656.12580)
- 649 30. Freeman, R. & Naumowicz, T. In press. MATAKI Tracking Devices. UCL CoMPLEX,  
 650 Zoological Society of London, Microsoft Research Cambridge.
- 651 31. Freeman, R., Shoji, A., Fayet, A., Dean, B., Kirk, H., Perrins, C. & Guilford, T. 2012  
 652 Tracking the migration and foraging dynamics of Lundy’s Manx shearwaters. *Lundy F.*  
 653 *Soc. Annu. Rep. 2012* , 101–106.
- 654 32. R Core Team 2014 R: A Language & Environment for Statistical Computing. R  
 655 Foundation for Statistical Computing, Vienna, Austria.
- 656 33. Calenge, C., Dray, S. & Royer-Carenzi, M. 2009 The concept of animals’ trajectories  
 657 from a data analysis perspective. *Ecol. Inform.* **4**, 34–41.  
 658 (doi:10.1016/j.ecoinf.2008.10.002)

- 659 34. Dray, S., Royer-Carenzi, M. & Calenge, C. 2010 The exploratory analysis of  
 660 autocorrelation in animal-movement studies. *Ecol. Res.* **25**, 673–681.  
 661 (doi:10.1007/s11284-010-0701-7)
- 662 35. Benhamou, S. 2004 How to reliably estimate the tortuosity of an animal's path:  
 663 straightness, sinuosity, or fractal dimension? *J. Theor. Biol.* **229**, 209–220.  
 664 (doi:10.1016/j.jtbi.2004.03.016)
- 665 36. Fraley, C. & Raftery, A. . 2002 Model-based clustering, discriminant analysis and density  
 666 estimation. *J. Am. Stat. Assoc.* **97**, 611–631. (doi:10.1198/016214502760047131)
- 667 37. Fraley, C., Raftery, A. ., Murphy, T. & Scrucca, L. 2012 mclust Version 4 for R: Normal  
 668 Mixture Modeling for Model-Based Clustering, Classification, and Density  
 669 Estimation. Technical Report No. 597, Department of Statistics, University of Washington.
- 670 38. Bates, D., Maechler, M., Bolker, B. & Walker, S. 2014 lme4: Linear mixed-effects models  
 671 using Eigen and S4. R package version 1.1-7.
- 672 39. Pante, E. & Simon-Bouhet, B. 2013 marmap: A Package for Importing, Plotting and  
 673 Analyzing Bathymetric and Topographic Data in R. *PLoS One* **8**, e73051.  
 674 (doi:10.1371/journal.pone.0073051)
- 675 40. Zhao, Q., Xu, M. & Fränti, P. 2008 Knee point detection on Bayesian information  
 676 criterion. *Proc. - Int. Conf. Tools with Artif. Intell. ICTAI* **2**, 431–438.  
 677 (doi:10.1109/ICTAI.2008.154)
- 678 41. Davies, R. G., Irlich, U. M., Chown, S. L. & Gaston, K. J. 2010 Ambient, productive and  
 679 wind energy, and ocean extent predict global species richness of procellariiform seabirds.  
 680 *Glob. Ecol. Biogeogr.* **19**, 98–110. (doi:10.1111/j.1466-8238.2009.00498.x)
- 681 42. Dean, B., Freeman, R., Kirk, H., Leonard, K., Phillips, R. A., Perrins, C. M. & Guilford,  
 682 T. 2012 Behavioural mapping of a pelagic seabird: combining multiple sensors and a  
 683 hidden Markov model reveals the distribution of at-sea behaviour. *J. R. Soc. Interface* ,

- 684 20120570. (doi:10.1098/rsif.2012.0570)
- 685 43. Vandenabeele, S. P., Grundy, E., Friswell, M. I., Grogan, A., Votier, S. C. & Wilson, R. P.  
686 2014 Excess baggage for birds: inappropriate placement of tags on gannets changes flight  
687 patterns. *PLoS One* **9**, e92657. (doi:10.1371/journal.pone.0092657)
- 688 44. Gleiss, A. C., Wilson, R. P. & Shepard, E. L. C. 2011 Making overall dynamic body  
689 acceleration work: on the theory of acceleration as a proxy for energy expenditure.  
690 *Methods Ecol. Evol.* **2**, 23–33. (doi:10.1111/j.2041-210X.2010.00057.x)
- 691 45. Wilson, R. P., White, C. R., Quintana, F., Halsey, L. G., Liebsch, N., Martin, G. R. &  
692 Butler, P. J. 2006 Moving towards acceleration for estimates of activity-specific metabolic  
693 rate in free-living animals: The case of the cormorant. *J. Anim. Ecol.* **75**, 1081–1090.  
694 (doi:10.1111/j.1365-2656.2006.01127.x)
- 695 46. Wilson, R. P., Quintana, F. & Hobson, V. J. 2012 Construction of energy landscapes can  
696 clarify the movement and distribution of foraging animals. *Proc. R. Soc. B* **279**, 975–80.  
697 (doi:10.1098/rspb.2011.1544)
- 698 47. Langston, R. H. W. 2010 Offshore wind farms and birds: Round 3 zones, extensions to  
699 Round 1 & Round 2 sites & Scottish Territorial Waters.
- 700 48. Paleczny, M., Hammill, E., Karpouzi, V. & Pauly, D. 2015 Population trend of the  
701 world's monitored seabirds, 1950-2010. *PLoS One* **10**, e0129342.  
702 (doi:10.1371/journal.pone.0129342)
- 703